Improved understanding of eutrophication trends, indicators and problem areas using machine learning

Deep S. Banerjee, Jozef Skákala

[1]Plymouth Marine Laboratory, Plymouth, UK
[2]National Centre for Earth Observation, Plymouth, UK

Key Points:

- Applying machine learning to observations we derive a gap-free, 7 km, daily, bi-decadal nitrate data-set for North-West European Shelf seas.
- We identify nitrate-limited areas across the domain that are vulnerable to eutrophication.
- We identify trends in nitrate concentrations corresponding to major riverine discharge changes over the last decades.

Corresponding author: Deep S. Banerjee, `dba@pml.ac.uk`

Abstract

Eutrophication is a reoccurring problem in coastal regions, including the North-West European Shelf (NWES). By developing machine learning model from sparse observations, we reconstruct a gap-free, 7km and daily, bi-decadal (1998-2020), data-set for nitrate at the NWES, allowing for much more robust analyses than the sparse observational data. From the data-set we identify nitrate-limited coastal areas, which are potentially vulnerable to eutrophication. Apart from known eutrophication-problem areas, these include additional coastal zones, which could become problematic under sub-optimal policy, or management changes. Furthermore, we show only a limited link between winter nitrate and the size of phytoplankton growth the following year, suggesting winter inorganic nitrogen might not provide the best indicator for eutrophication (as used by OSPAR). Finally, we demonstrate that reduction of nitrate on the NWES in the 1998-2020 period has been mostly small, with the exception of specific areas, such as the Bay of Biscay.

Plain Language Summary

Nitrate is an essential inorganic nutrient limiting phytoplankton growth in many marine environments. Nutrient pollution, e.g. from agriculture, can cause uncontrolled growth of algae (called eutrophication events), with serious consequences for marine ecosystem health. A region, essential for economy and carbon sequestration, historically impacted by such events, is the North-West European Shelf (NWES). Nitrate observations on the NWES are difficult to obtain and thus sparse both in time and space. We demonstrate that machine learning can generate, from sparse observations, a skilled, gap-free, bi-decadal surface nitrate data-set on a daily and 7km scale. With such a data-set we can address questions that would be otherwise hard to answer: (i) We show that nitrate-limited regions on the NWES, potentially vulnerable to eutrophication, extend beyond the eutrophication-problem areas already identified by the monitoring bodies (i.e. OSPAR). (ii) We demonstrate that bi-decadal 1998-2020 trends in coastal nitrate, responding to long-term policy-driven reduction in riverine discharge, are mostly modest with a notable exception of the Bay of Biscay. (iii) We show that winter nitrate plays relatively minor direct role in the phytoplankton bloom intensity the following spring, which can have some implications for using winter inorganic nitrogen as eutrophication indicator (as is relatively common).

1 Introduction

Nitrogen is one of the most important components of organic matter, needed in relatively large concentrations, as demonstrated by the Redfield ratios (Tett et al., 1985). Despite of its large abundance (the Earth's atmosphere comprises 78% nitrogen as N_2), it is non-trivial to obtain nitrogen in forms useful for plants. As a consequence of this, nitrogen is often the most limiting nutrient for plant, or algae growth, including the coastal marine environment (Ryther & Dunstan, 1971; Board et al., 2000). Nitrogen fixation, converting atmospheric nitrogen to forms useful for life, happens through various biotic and abiotic pathways, resulting in ammonium, nitrite and nitrate (Noxon, 1976; Hill et al., 1980; Postgate, 1998; Beman et al., 2008; Voss et al., 2013). Nitrate in the ocean is the primary nutrient for phytoplankton, with phytoplankton uptake enabling nitrogen flows into higher trophic levels and various detrital and dissolved forms of organic matter. In a nitrogen-limited environment, excess nitrate concentrations, primarily originating from agricultural runoff and industrial wastewater discharge, can stimulate harmful eutrophication events (Withers et al., 2014; Nazari-Sharabian et al., 2018). The thick layer of algae produced by these events may cut oxygen ventilation at the surface and after the algae die off and sink, the decomposers may consume vast amounts of oxygen, leading to marine hypoxia in the bottom part of the water column (Rabalais et al., 2002;

Diaz & Rosenberg, 2008). Furthermore, eutrophication events are often dominated by species that produce toxins that have detrimental effects on the marine ecosystem by causing fish kills, seafood contamination, and even posing risks to human lives (Anderson et al., 2012). Additionally, high nitrate concentrations lead to the excessive production of organic matter, which, upon decomposition, increases CO_2 concentration, contributing to ocean acidification (Doney et al., 2009). Eutrophication is a fundamental problem in many shelf sea and coastal areas (Rabalais et al., 2009), with nitrate monitoring and predicting providing an essential tool informing marine management and policy.

An important region, subject to eutrophication, is the North-West European Shelf (NWES). NWES is impacted by significant river inputs, notably the Thames, Rhine, and Loire, which introduce substantial freshwater and nutrients into the region, influencing salinity and water properties. Open ocean shelf exchange, especially transport of nutrients and carbon across the shelf break, play another vital role in the NWES ecosystem dynamics (Huthnance et al., 2009). NWES has high ecological importance due to its high biological productivity, underpinning significant commercial fisheries and carbon sequestration (Pauly et al., 2002; Borges et al., 2006; Jahnke, 2010). During the 1980s, the NWES, particularly near the German Bights and the Westerschelde estuary, experienced notable shifts in nutrient distribution, primarily driven by increased continental nutrient inputs. Riverine discharges, particularly from the Rhine and Elbe, have been identified as major contributors to nutrient dynamics in the region (Brockmann & Eberlein, 1986; Radach, 1992), having adverse effects on the local ecosystem. However, EU regulations set by OSPAR convention in 1992 substantially decreased the nitrate deposition into the NWES (Burson et al., 2016).

The NWES nitrate concentrations are operationally simulated and predicted (Skákala et al., 2018), however, the NWES nitrate observations are too sparse to properly constrain the simulated nitrate through data assimilation. The current operational NWES system is mainly constrained by the much more robust satellite temperature and chlorophyll observations (Skákala et al., 2018, 2021, 2022) and avoids assimilating nutrients entirely. Furthermore, due to its univariate nature, the operational system fails to directly constrain most of the non-assimilated variables including nutrients. Consequently, the nitrate reanalyses and forecasts produced by the operational system are known to have substantial biases, inherited from the model free run (Skákala et al., 2018, 2022). Although the simulated physics and chlorophyll from the reanalysis validate well against observations (Skákala et al., 2018, 2022), the nitrate NWES product is of more limited use.

In this work we develop and validate a new bi-decadal NWES nitrate product derived from the available observations using advanced machine learning (ML) algorithms. The nitrate product is developed for the ocean surface, where nutrients have the potential to most significantly drive phytoplankton growth. This is up to our knowledge the by far most complete and detailed observation-based sea surface nitrate data-set on the NWES. Unlike the NWES operational reanalysis, the data-set validates skillfully against the independent observations. Using our NWES nitrate product we are able to discuss several important questions, like the impact of winter nitrate pre-conditioning on the interannual phytoplankton variability, identify the NWES geographic areas limited by nitrate, or analyse trends in nitrate concentrations on the NWES. To do so, we maximise our reliance on the observational data and use ML and modelling to effectively fill the large data-gaps, either through statistics, or dynamical consistency imposed by deterministic modelling.

2 Methodology

The details on data and ML model architecture can be found in the Supporting Information (SI), Sec.1-2. Here we offer the reader just a short summary.

We used as the ML model a Feed-forward Neural Network (NN) designed through the Autokeras library using a Structured Data Regressor (Jin et al., 2019). The model used a number of input features for nitrate prediction: (i) structural data, such as latitude, longitude, day/month, depth and bathymetry, (ii) physical and biogeochemical variables obtained from the 1998-2020, daily and 7km resolution, Copernicus NWES reanalysis (Kay et al. (2016), for its components see also Brewin et al. (2010, 2017); Skákala et al. (2018); Madec et al. (2017); Bruggeman and Bolding (2014); Butenschön et al. (2016)): sea surface temperature (SST), total surface phytoplankton chlorophyll and carbon, total surface net primary production, as well as surface chlorophyll of four phytoplankton functional types (PFTs), i.e. diatoms, microphytoplankton, nanophytoplankton and picophytoplankton, (iii) SST observations from the Global Ocean OSTIA product (Good et al., 2020; Donlon et al., 2012), (iv) daily riverine discharge data from an updated version of the river dataset (Lenhart et al., 2010), (v) ERA-5, daily-averaged and 0.25°, atmospheric reanalysis data (Hersbach et al., 2020) for downwelling shortwave radiation at the ocean surface, specific humidity, temperature and dew point temperature at 2m above the ocean surface, total precipitation, zonal and meridional wind components at 10m above the ocean surface (these can act as proxies for atmospheric fluxes of nitrogen into the ocean (Duce et al., 2008)). All the input features were considered at the same times than the predicted nitrate. To avoid biases towards operational models, the NN model input features were always selected to be either observational data, or reanalyses of variables closely constrained by the observations. The relative importance of the input features was evaluated by the SHAP analysis (Linardatos et al., 2020) and is presented in Fig.S2 of SI.

The nitrate data were obtained from the International Council for the Exploration of the Sea (ICES) Dataportal https://www.ices.dk. The NN model inputs were interpolated into the ICES data locations, and then the ICES data from the 1998-2015 period, containing 43572 relevant data-points (see Fig.S3 of SI), were used for training and validation of the NN model (with 80% data used for training and 20% used for validation). Finally, the 2016-2018 ICES data, containing 2984 data-points (Fig.S3 of SI), were used as test data. We have also validated the model with other independent test data (i) from the L4 station of the Western Channel Observatory (Harris, 2010), as well as from (ii) five stations of the Scottish Coastal Observatory (Bresnan et al., 2016; Hindson et al., 2018). Finally, after validating the NN model, we have run it for the full 1998-2020 period across the whole Copernicus NWES reanalysis domain (see Fig.1), taking Copernicus reanalysis, river and ERA-5 atmospheric forcing inputs and producing a gap-free bi-decadal, daily, 7 km resolution reconstruction of nitrate. This final data-set underpins the results from this study.

3 Results and discussion

3.1 Model validation

Fig.2, Tab.1 and Fig.S5-S6 of SI demonstrate that the NN model shows a very good skill relative to the test data from ICES, L4 and the Scottish stations, and substantially outperforms the existing Copernicus reanalysis product for NWES nitrate.

Because the nitrate time series are dominated by the seasonal signal, it is important to explore whether the model skill extends beyond predicting the local nitrate seasonal (e.g. monthly) climatology. This is much harder to validate, as one needs long term time-series at specific locations, which are rare. We have looked at the data from the L4 station and five Scottish locations to analyse the ML model skill to capture interannual variability of nitrate. The results (shown in Tab.1 and Fig.S7 of SI) are more mixed: at L4 station, which has from all the locations the longest time-record and richest data-set, the ML model performs very well in predicting the inter-annual nitrate time-series. It is interesting that at the same location the reanalysis does a very poor job in doing the

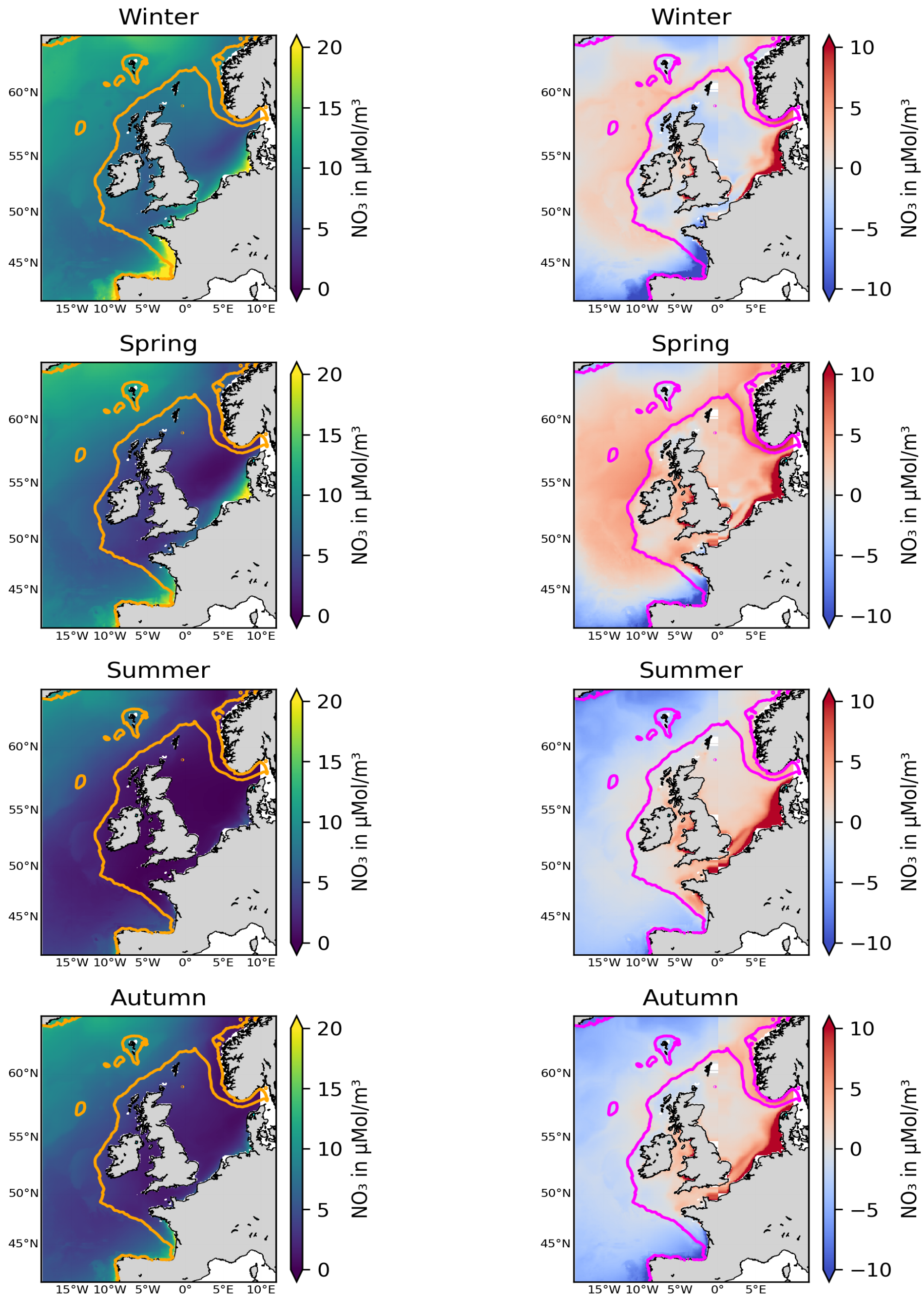

Figure 1. The left-hand panels show the NN-reconstructed 1998-2020 average surface nitrate concentrations for different annual seasons. The right-hand panels show the same averages for the relative bias of the Copernicus surface nitrate reanalysis (Kay et al., 2016) with respect to the NN-reconstructed data-set (reanalysis minus NN-reconstructed). The contours mark NWES (bathymetry<200m).

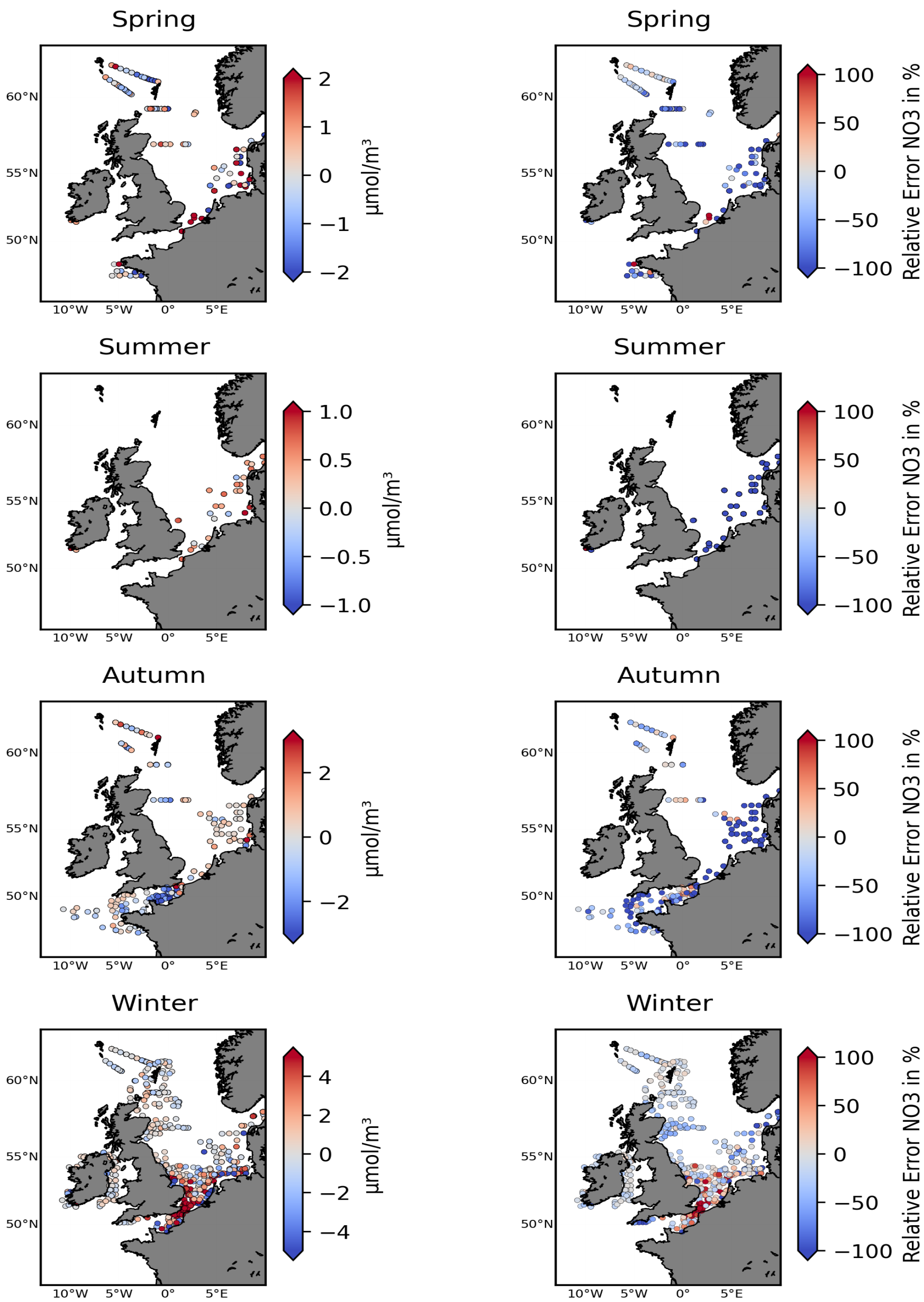

Figure 2. The left-hand panels show the ICES nitrate test data locations for different seasons, with the colorbar accounting for the NN-model skill (difference between predicted and observed nitrate: predicted - observed). The right-hand panel shows the relative differences between the NN model and the Copernicus reanalysis skill as defined in Eq.1 of SI. It marks an NN-model improvement (blue), or degradation (red) relative to the reanalysis, when compared (in %) to the observed nitrate concentrations.

Table 1. The skill of the NN model in predicting nitrate compared with the Copernicus reanalysis (Kay et al., 2016). Skill is measured by bias (Eq.2 of SI, in μmol/m^3), Bias-Corrected Root Mean Squared Error (BC-RMSE, Eq.3 of SI, in μmol/m^3) and Pearson correlation. The rows represent different test data from ICES and the coastal stations (see Sec.1 and Fig.S1 of SI). The last two rows show the skill of the NN model and the reanalysis to predict interannual, low-pass filtered time-series (for details see Fig.S7 of SI). For the five Scottish stations we show only the averaged result through all the stations.

	NN predicted			**Reanalysis**		
Test data	**bias**	**BC-RMSE**	**R**	**bias**	**BC-RMSE**	**R**
ICES	0.62	2.37	0.72	3.18	6.15	0.27
L4	-1.03	1.85	0.79	0.20	2.22	0.72
Scalloway	0.98	2.1	0.8	1.08	2.76	0.64
St.Abbs	-0.25	1.25	0.9	0.73	1.87	0.85
Scapa	1.52	1.52	0.86	0.33	2.13	0.69
Stonehaven	-0.53	0.97	0.95	0.09	2.04	0.78
Loch Ewe	1.57	0.92	0.93	0.57	1.1	0.89
L4 interannual	–	0.72	0.52	–	0.99	0.08
Scottish interannual	–	0.512	-0.144	–	0.756	0.204

same (Tab.1). At the Scottish stations the ML model correctly captures the size of the interannual variability in nitrate, whereas struggles to capture the variability itself (the R metrics in Tab.1). It is however noteworthy that some of the time-series at the Scottish locations are relatively short (see Sec.1 of SI) and therefore not the most suitable for this type of analysis.

Finally, the test data selected from the ICES data-set are time-separated from the training and validation data, but were spatially located in largely overlapping regions (see Fig.S3 of SI). It is therefore important to explore the possibility that, due to geographic proximity, some ML skill has been transferred from the training/validation data to the test data. This is done in Fig.S8 of SI, showing how the skill evolves as a function of spatial separation between the test data and the training/validation data. Although there is large variability in the skill, Fig.S8 shows no significant trend with spatial distance, indicating that the ML model skill does not decrease (even slightly improves) with the increase in spatial separation.

3.2 The bi-decadal nitrate product, the trends, variability and implications

Fig.1 shows the 1998-2020 seasonally averaged NWES nitrate concentrations. It is clear from the spatial nitrate distributions that the ML model does not capture sufficiently the ∼7km scale variability, including the exact NWES boundaries, but it does reasonably capture coarse resolution nitrate distributions (see Fig.S9 of SI for comparison with the WOA product (Garcia et al., 2019)). Similarly, our analyses (including Fig.S4 and Fig.S6) suggest that the effective temporal resolution of the NN product is ∼15-day, rather than daily. Fig.1 also provides seasonal comparison with the Copernicus reanalysis product, evaluating the significant reanalysis biases throughout the 1998-2020 period. The Copernicus reanalysis validation gives similar results to validation from Kay et al. (2016), who compared the reanalysis with the North Sea Biogeochemical 1960-2014 Climatology (Hinrichs et al., 2017).

The winter nitrate concentrations play an important role in pre-conditioning of the spring bloom, which largely drives the NWES biogeochemical seasonal cycles (Huisman et al., 1999; He et al., 2011). The winter total inorganic nitrogen is used by OSPAR, in combination with other parameters, using Common Procedure (OSPAR, 2005), as an important indicator for NWES eutrophication and next season's growth (Axe et al., 2017; Topcu & Brockmann, 2021). The hypothesis, that the intensity of spring phytoplankton bloom is directly related to the abundance of nutrients in the winter before the bloom, has been investigated here through nitrate. In Fig.3:A we have found only limited evidence for the relationship between the winter nitrate abundance and spring bloom intensity, i.e. statistically significant positive Pearson correlation has been found only in the western English Channel region, near the shelf-break in the Celtic Sea, around the Bay of Biscay and in the south-west of the model domain (accounting at most for 30-35% of explained variance). Fig.3:A also shows that these are regions where the inter-annual nitrate variability appears to be relatively large (10-20% of the winter average, Fig.3:B) and therefore capable to reveal stronger relationship with spring chlorophyll. For most of the domain, there is lack of clear correlation between inter-annual winter nitrate and spring chlorophyll, which could be explained by the fact that both are driven by the interannual variability in the atmosphere (Dutkiewicz et al., 2001; Follows & Dutkiewicz, 2001; Ueyama & Monger, 2005; Henson et al., 2006; Zhai et al., 2013). Increased winds can lead to more mixing and elevated surface nutrients, whilst dampening blooms by transporting phytoplankton below the Sverdrup critical depth, as proposed by popular hypotheses explaining the North Atlantic spring blooms (Sverdrup, 1953; Huisman et al., 1999). Furthermore, there is lack of complete agreement on what are the dominant drivers of the spring bloom in the North Atlantic, and arguments have been raised supporting the view that blooms result much more from the internal ecosystem dynamics (e.g. zooplankton control over phytoplankton, Behrenfeld and Boss (2014)), compared to what was assumed by the traditional hypotheses focusing on physics.

In Fig.3:C we look at correlations between inter-annual time-series of summer nitrate and chlorophyll concentrations, indicating areas where phytoplankton is nitrate-limited (these are displayed by positive correlation). The Fig.3:C shows that chlorophyll is nitrate-limited mostly in the southern North Sea region, in the western English Channel, Bay of Biscay and the south-west of the domain. These are again the regions where the inter-annual fluctuations of summer nitrate are relatively large (Fig.3:D). The nitrate-limitation in these areas means they are vulnerable to eutrophication, if excess of nutrients is introduced into the water. Indeed, it is re-assuring that the eutrophication-problem areas, as identified by the OSPAR NWES eutrophication status reports (such as south-eastern North Sea, coastal areas around Brittany, Axe et al. (2017)), fall under these vulnerable zones delimited in Fig.3:C. However, Fig.3:C includes also other regions, such as eastern coastline of Scotland, southern coast of Ireland and zones in the Irish Sea. Our results indicate that these additional regions could easily become problem-areas, if the policy and management of agriculture runoff became less effective.

Finally Fig.4, shows 1998-2020 trends in winter nitrate across the NWES domain. In most of the domain no statistically significant nitrate trends have been detected, but some small negative trends ($\sim$0.02 μmol/(m^3.year)) were found in the Southern North Sea and the north-east region near the Norwegian trench. Somewhat larger ($\sim$0.08 μmol/-(m^3.year)) statistically significant negative trends have been found in specific locations of the Bay of Biscay. These results (e.g. from the Southern North Sea) are broadly consistent with what has been reported for this period in the recent OSPAR report (e.g.Axe et al. (2017)). These small trends follow the smaller rates of reduction in the nitrate river-

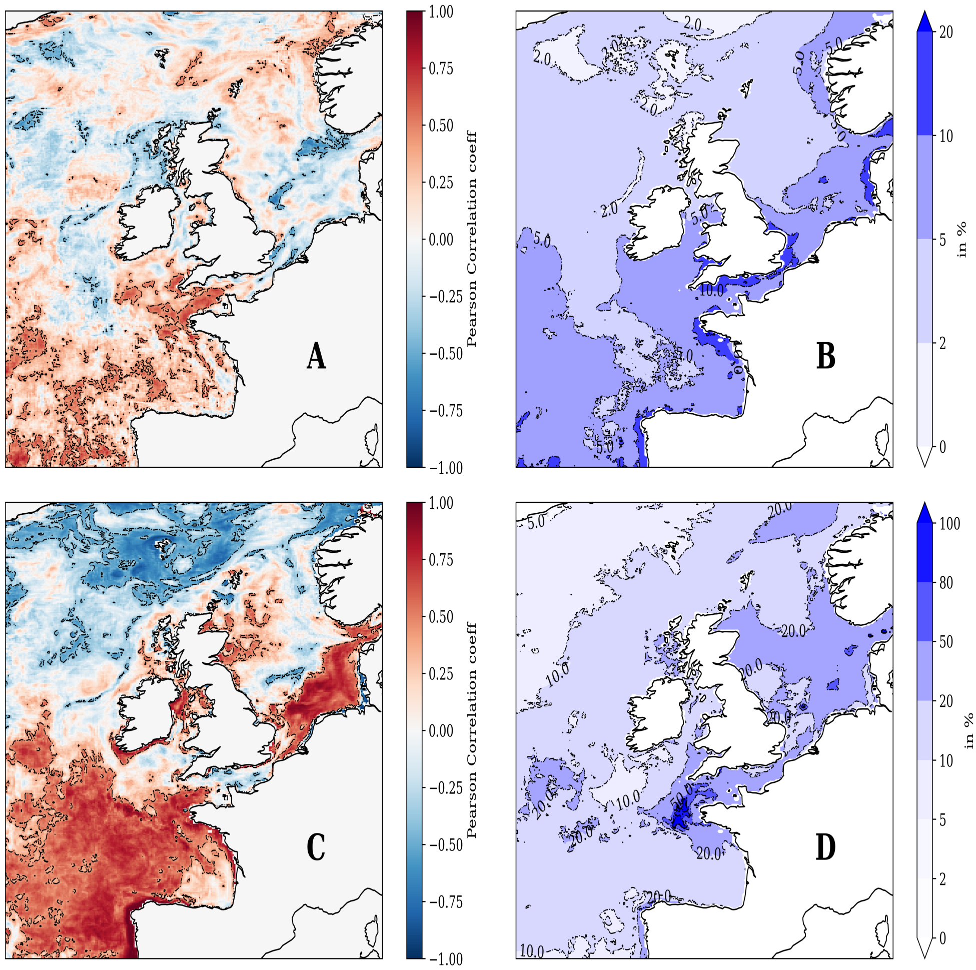

Figure 3. The upper left-hand panel (A) shows the Pearson correlation between the mean winter surface nitrate concentrations and the mean (following) spring surface chlorophyll concentration from the Copernicus reanalysis. The upper right-hand panel (B) shows the inter-annual variability for winter surface nitrate (across 1998-2020, measured by the standard deviation), relative to the 1998-2020 winter mean (in %). The bottom left panel (C) is similar to panel A, but showing the Pearson correlation between the summer surface nitrate and the summer surface total chlorophyll. The panel D is the same as the panel B, but showing inter-annual variability of surface nitrate in the summer, rather than winter. The dashed contours in panels A and C show regions where the correlation is statistically significant (p-value<0.05).

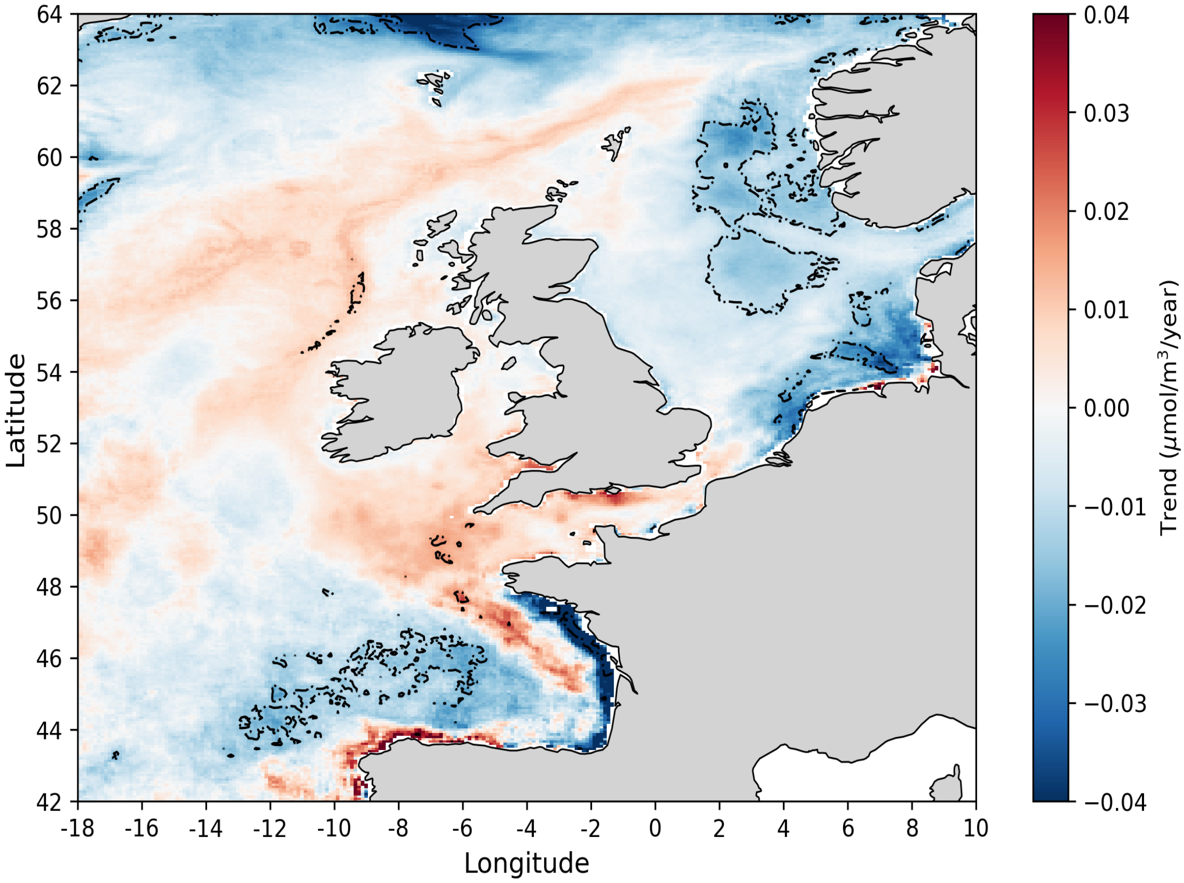

Figure 4. Linear trends at each spatial location in the annual nitrate 1998-2020 time-series. Dashed contours mark areas with statistically significant (p-value<0.05) trends.

ine inputs during the data period (1998-2020), compared to their large reduction in the 1980's and earlier 1990's (Duarte, 2009; Brockmann et al., 2018; Greenwood et al., 2019).

4 Conclusions

In this work we have demonstrated that, using sparse observations across the NWES, ML can provide a powerful tool to reconstruct spatially complete sea surface nitrate data-set over 22 year period. We have shown that the data-set has substantially better match-ups with independent test data than the existing NWES nitrate reanalysis. Using the newly developed product, we have identified nitrate-limited areas potentially vulnerable to eutrophication, addressed nitrate decadal trends, and tested how successfully winter nitrate can be used as a predictor of the phytoplankton spring bloom. There are many other potential scientific uses of the nitrate data-set, e.g. we propose to assimilate the nitrate data into the NWES operational model, correcting the model significant nitrate biases, potentially improving its dynamics and its short-range forecasts. The model skill in simulating phytoplankton is known to quickly degrade with the forecast lead time (e.g.

Kay et al. (2016); Skákala et al. (2018)) and biases in nitrate might be one of the leading factors in driving this.

Several extensions of this work would be also desirable, such as utilizing ICES data for other biogeochemical indicators to produce ML-informed multi-variate data-sets across the whole NWES domain (these should include other nutrients and oxygen). ML could also identify valuable patterns of relationships across the multiple variables. Furthermore, the model developed here did not show very good skill in capturing high-frequency (daily) temporal variability, including extreme events. This might be due to processes providing ocean with memory significantly longer than the daily time-scale of the product. Representing ocean memory by the NN model might require using time-lagged input features, which could substantially inflate the size and the complexity of the model. Despite of that, including such features into the NN model should be considered in the future. Finally, ML tools designed to specifically capture extreme phenomena can be deployed in the future and extend the applicability of this work.

Acknowledgments

This work was funded by the Horizon Europe project The New Copernicus Capability for Tropic Ocean Networks (NECCTON, grant agreement no.101081273). We also acknowledge support from the UK NERC single centre national capability programme – CLASS (NE/R015953/1). We used in this study the atmospheric ERA5 product of the ECMWF (https://www.ecmwf.int/), as well as river data prepared by Sonja van Leeuwen and Helen Powley as part of UK SSB programme (contract no.NE/K001876/1) of the NERC and the DEFRA. The riverine data contained also climatological values from the Global River Discharge Data Base and the Centre for Ecology and Hydrology (Young & Holt, 2007). We have also used EU Copernicus reanalyses; the NWSHELF_MULTIYEAR_BGC_004_011 (https://doi.org/10.48670/moi-00059) product for biogeochemistry, and NWSHELF_MULTIYEAR_PHY_004_009 (https://doi.org/10.48670/moi-00058) for physics. We have used nitrate data-sets from the ICES portal, from the Western Channel Observatory, and the Scottish Coastal Observatory. We would like to thank Jerry Blackford, Gennadi Lessin, Yuri Artioli, Helen Powley, Bee Berx and Julien Brajard for comments and discussions.

5 Open Research.

All the data used here can be publicly downloaded from EU Copernicus (https://doi.org/10.48670/moi-00058), ICES portal (https://doi.org/10.17895/ices.pub.8883), Western Channel Observatory (https://www.westernchannelobservatory.org.uk/l4_nutrients.php) and the Scottish Coastal Observatory (doi:10.7489/610-1, doi:10.7489/953-1, doi:10.7489/952-1, doi:10.7489/948-1, doi:10.7489/12138-1). The ML software is placed in https://github.com/neccton-algo.

References

Anderson, D. M., Cembella, A. D., & Hallegraeff, G. M. (2012). Progress in understanding harmful algal blooms: paradigm shifts and new technologies for research, monitoring, and management. *Annual review of marine science*, *4*, 143–176.

Axe, P., Clausen, U., Leujak, W., Malcolm, S., & Harvey, E. (2017). Eutrophication status of the ospar maritime area. *Third Integrated Report on the Eutrophication Status of the OSPAR Maritime Area*.

Behrenfeld, M. J., & Boss, E. S. (2014). Resurrecting the ecological underpinnings of ocean plankton blooms. *Annual review of marine science*, *6*, 167–194.

Beman, J. M., Popp, B. N., & Francis, C. A. (2008). Molecular and biogeochemical evidence for ammonia oxidation by marine crenarchaeota in the gulf of california. *The ISME Journal*, *2*(4), 429–441.

Board, O. S., Council, N. R., et al. (2000). *Clean coastal waters: understanding and reducing the effects of nutrient pollution.* National Academies Press.

Borges, A., Schiettecatte, L.-S., Abril, G., Delille, B., & Gazeau, F. (2006). Carbon dioxide in european coastal waters. *Estuarine, Coastal and Shelf Science*, *70*(3), 375–387.

Bresnan, E., Cook, K., Hindson, J., Hughes, S., Lacaze, J., Walsham, P., . . . Turrell, W. (2016). The scottish coastal observatory 1997–2013. part 2-description of scotland's coastal waters. *Scottish Marine and Freshwater Science*, *7*(26).

Brewin, R. J., Ciavatta, S., Sathyendranath, S., Jackson, T., Tilstone, G., Curran, K., . . . others (2017). Uncertainty in ocean-color estimates of chlorophyll for phytoplankton groups. *Frontiers in Marine Science*, *4*, 104.

Brewin, R. J., Sathyendranath, S., Hirata, T., Lavender, S. J., Barciela, R. M., & Hardman-Mountford, N. J. (2010). A three-component model of phytoplankton size class for the atlantic ocean. *Ecological Modelling*, *221*(11), 1472–1483.

Brockmann, U., & Eberlein, K. (1986). River input of nutrients into the german bight. In *The role of freshwater outflow in coastal marine ecosystems* (pp. 231–240). Springer.

Brockmann, U., Topcu, D., Schütt, M., & Leujak, W. (2018). Eutrophication assessment in the transit area german bight (north sea) 2006–2014–stagnation and limitations. *Marine pollution bulletin*, *136*, 68–78.

Bruggeman, J., & Bolding, K. (2014). A general framework for aquatic biogeochemical models. *Environmental modelling & software*, *61*, 249–265.

Burson, A., Stomp, M., Akil, L., Brussaard, C. P., & Huisman, J. (2016, 5). Unbalanced reduction of nutrient loads has created an offshore gradient from phosphorus to nitrogen limitation in the north sea. *Limnology and Oceanography*, *61*, 869-888. doi: 10.1002/LNO.10257

Butenschön, M., Clark, J., Aldridge, J. N., Allen, J. I., Artioli, Y., Blackford, J., . . . others (2016). Ersem 15.06: a generic model for marine biogeochemistry and the ecosystem dynamics of the lower trophic levels. *Geoscientific Model Development*, *9*(4), 1293–1339.

Diaz, R. J., & Rosenberg, R. (2008). Spreading dead zones and consequences for marine ecosystems. *science*, *321*(5891), 926–929.

Doney, S. C., Fabry, V. J., Feely, R. A., & Kleypas, J. A. (2009). Ocean acidification: the other co2 problem. *Annual review of marine science*, *1*, 169–192.

Donlon, C. J., Martin, M., Stark, J., Roberts-Jones, J., Fiedler, E., & Wimmer, W. (2012). The operational sea surface temperature and sea ice analysis (ostia) system. *Remote Sensing of Environment*, *116*, 140–158.

Duarte, C. M. (2009). Coastal eutrophication research: a new awareness. In *Eutrophication in coastal ecosystems: Towards better understanding and management strategies selected papers from the second international symposium on research and management of eutrophication in coastal ecosystems, 20–23 june 2006, nyborg, denmark* (pp. 263–269).

Duce, R. A., LaRoche, J., Altieri, K., Arrigo, K. R., Baker, A. R., Capone, D., . . . others (2008). Impacts of atmospheric anthropogenic nitrogen on the open ocean. *Science*, *320*(5878), 893–897.

Dutkiewicz, S., Follows, M., Marshall, J., & Gregg, W. W. (2001). Interannual variability of phytoplankton abundances in the north atlantic. *Deep Sea Research Part II: topical studies in oceanography*, *48*(10), 2323–2344.

Follows, M., & Dutkiewicz, S. (2001). Meteorological modulation of the north atlantic spring bloom. *Deep Sea Research Part II: Topical Studies in Oceanography*, *49*(1-3), 321–344.

Garcia, H., Weathers, K., Paver, C., Smolyar, I., Boyer, T., Locarnini, M., . . . others (2019). World ocean atlas 2018. vol. 4: Dissolved inorganic nutrients

(phosphate, nitrate and nitrate+ nitrite, silicate).
Good, S., Fiedler, E., Mao, C., Martin, M. J., Maycock, A., Reid, R., … others (2020). The current configuration of the ostia system for operational production of foundation sea surface temperature and ice concentration analyses. *Remote Sensing*, *12*(4), 720.
Greenwood, N., Devlin, M. J., Best, M., Fronkova, L., Graves, C. A., Milligan, A., … Van Leeuwen, S. M. (2019). Utilizing eutrophication assessment directives from transitional to marine systems in the thames estuary and liverpool bay, uk. *Frontiers in Marine Science*, *6*, 116.
Harris, R. (2010). The l4 time-series: the first 20 years. *Journal of Plankton Research*, *32*(5), 577–583.
He, R., Chen, K., Fennel, K., Gawarkiewicz, G., & McGillicuddy Jr, D. (2011). Seasonal and interannual variability of physical and biological dynamics at the shelfbreak front of the middle atlantic bight: nutrient supply mechanisms. *Biogeosciences*, *8*(10), 2935–2946.
Henson, S. A., Robinson, I., Allen, J. T., & Waniek, J. J. (2006). Effect of meteorological conditions on interannual variability in timing and magnitude of the spring bloom in the irminger basin, north atlantic. *Deep Sea Research Part I: Oceanographic Research Papers*, *53*(10), 1601–1615.
Hersbach, H., Bell, B., Berrisford, P., Hirahara, S., Horányi, A., Muñoz-Sabater, J., … others (2020). The era5 global reanalysis. *Quarterly Journal of the Royal Meteorological Society*, *146*(730), 1999–2049.
Hill, R., Rinker, R., & Wilson, H. D. (1980). Atmospheric nitrogen fixation by lightning. *Journal of Atmospheric Sciences*, *37*(1), 179–192.
Hindson, J., Berx, B., Hughes, S., Walsham, P., Machairpoulou, M., Bresnan, E., & Turrell, B. (2018). The scottish coastal observatory. *Bollettino di Geofisica*, 333.
Hinrichs, I., Gouretski, V., Pätch, J., Emeis, K., & Stammer, D. (2017). North sea biogeochemical climatology.
Huisman, J., van Oostveen, P., & Weissing, F. J. (1999). Critical depth and critical turbulence: two different mechanisms for the development of phytoplankton blooms. *Limnology and oceanography*, *44*(7), 1781–1787.
Huthnance, J. M., Holt, J. T., & Wakelin, S. L. (2009). Deep ocean exchange with west-european shelf seas. *Ocean Science*, *5*(4), 621–634.
Jahnke, R. A. (2010). Global synthesis1. In *Carbon and nutrient fluxes in continental margins: A global synthesis* (pp. 597–615). Springer.
Jin, H., Song, Q., & Hu, X. (2019). Auto-keras: An efficient neural architecture search system. In *Proceedings of the 25th acm sigkdd international conference on knowledge discovery & data mining* (pp. 1946–1956).
Kay, S., McEwan, R., & Ford, D. (2016). North west european shelf production centre nwshelf_multiyear_bio_004_011. *CMEMS Report*, *3*, 21.
Lenhart, H.-J., Mills, D. K., Baretta-Bekker, H., Van Leeuwen, S. M., Van Der Molen, J., Baretta, J. W., … others (2010). Predicting the consequences of nutrient reduction on the eutrophication status of the north sea. *Journal of Marine Systems*, *81*(1-2), 148–170.
Linardatos, P., Papastefanopoulos, V., & Kotsiantis, S. (2020). Explainable ai: A review of machine learning interpretability methods. *Entropy*, *23*(1), 18.
Madec, G., Bourdallé-Badie, R., Bouttier, P.-A., Bricaud, C., Bruciaferri, D., Calvert, D., … others (2017). Nemo ocean engine.
Nazari-Sharabian, M., Ahmad, S., & Karakouzian, M. (2018). Climate change and eutrophication: a short review. *Engineering, Technology and Applied Science Research*, *8*(6), 3668.
Noxon, J. (1976). Atmospheric nitrogen fixation by lightning. *Geophysical Research Letters*, *3*(8), 463–465.

OSPAR, C. (2005). Common procedure for the identification of the eutrophication status of the ospar maritime area. *OSPAR Commission*, *3*.

Pauly, D., Christensen, V., Guénette, S., Pitcher, T. J., Sumaila, U. R., Walters, C. J., ... Zeller, D. (2002). Towards sustainability in world fisheries. *Nature*, *418*(6898), 689–695.

Postgate, J. R. (1998). *Nitrogen fixation.* Cambridge University Press.

Rabalais, N. N., Turner, R. E., Díaz, R. J., & Justić, D. (2009). Global change and eutrophication of coastal waters. *ICES Journal of Marine Science*, *66*(7), 1528–1537.

Rabalais, N. N., Turner, R. E., & Wiseman Jr, W. J. (2002). Gulf of mexico hypoxia, aka "the dead zone". *Annual Review of ecology and Systematics*, *33*(1), 235–263.

Radach, G. (1992). Ecosystem functioning in the german bight under continental nutrient inputs by rivers. *Estuaries*, *15*, 477–496.

Ryther, J. H., & Dunstan, W. M. (1971). Nitrogen, phosphorus, and eutrophication in the coastal marine environment. *Science*, *171*(3975), 1008–1013.

Skákala, J., Bruggeman, J., Ford, D., Wakelin, S., Akpınar, A., Hull, T., ... others (2022). The impact of ocean biogeochemistry on physics and its consequences for modelling shelf seas. *Ocean Modelling*, *172*, 101976.

Skákala, J., Ford, D., Brewin, R. J., McEwan, R., Kay, S., Taylor, B., ... Ciavatta, S. (2018). The assimilation of phytoplankton functional types for operational forecasting in the northwest european shelf. *Journal of Geophysical Research: Oceans*, *123*(8), 5230–5247.

Skákala, J., Ford, D., Bruggeman, J., Hull, T., Kaiser, J., King, R. R., ... others (2021). Towards a multi-platform assimilative system for north sea biogeochemistry. *Journal of Geophysical Research: Oceans*, *126*(4), e2020JC016649.

Sverdrup, H. U. (1953). On conditions for the vernal blooming of phytoplankton. *J. Cons. Int. Explor. Mer*, *18*(3), 287–295.

Tett, P., Droop, M. R., & Heaney, S. I. (1985). The redfield ratio and phytoplankton growth rate. *Journal of the Marine Biological Association of the United Kingdom*, *65*(2), 487–504. doi: 10.1017/S0025315400050566

Topcu, D., & Brockmann, U. (2021). Consistency of thresholds for eutrophication assessments, examples and recommendations. *Environmental Monitoring and Assessment*, *193*, 1–15.

Ueyama, R., & Monger, B. C. (2005). Wind-induced modulation of seasonal phytoplankton blooms in the north atlantic derived from satellite observations. *Limnology and Oceanography*, *50*(6), 1820–1829.

Voss, M., Bange, H. W., Dippner, J. W., Middelburg, J. J., Montoya, J. P., & Ward, B. (2013). The marine nitrogen cycle: recent discoveries, uncertainties and the potential relevance of climate change. *Philosophical Transactions of the Royal Society B: Biological Sciences*, *368*(1621), 20130121.

Withers, P. J., Neal, C., Jarvie, H. P., & Doody, D. G. (2014). Agriculture and eutrophication: where do we go from here? *Sustainability*, *6*(9), 5853–5875.

Young, E., & Holt, J. (2007). Prediction and analysis of long-term variability of temperature and salinity in the irish sea. *Journal of Geophysical Research: Oceans*, *112*(C1).

Zhai, L., Platt, T., Tang, C., Sathyendranath, S., & Walne, A. (2013). The response of phytoplankton to climate variability associated with the north atlantic oscillation. *Deep Sea Research Part II: Topical Studies in Oceanography*, *93*, 159–168.